Investigation of Propyphenazone Molecule by Quantum Chemical Methods

Öznur Büyük, Hanifi Kebiroglu*, Niyazi Bulut

Department of Physics, Faculty of Science, Firat University, 23119 Elazig, Türkiye
Corresponding author: E-mail: hanifi007@hotmail.com

ABSTRACT

Computational chemistry approaches were used to manage the phenazone molecule. The phenazone molecule was optimized at the 3-21G (d) level. The structural parameters were investigated. IR and NMR techniques, which are spectroscopic approaches, were used to determine the structure. The highest occupied molecular orbital (HOMO) energy, the lowest unoccupied molecular orbital (LUMO) energy, hardness (η), softness (σ), chemical potential (μ), electronegativity (χ), electrophilicity index (ω), nucleophilicity index (ε), the electron accepting power (ω+), electron-donating power (ω-), and polarizability of the propyphenazone molecule were investigated. NMR spectra for 1H and 13C, as well as UV-Vis spectra were obtained. HOMO-LUMO and molecular electrostatic potential (MEP) analyses were carried out. The theoretical calculations for the molecular structure and spectroscopy were done using the Gaussian 09 software with HF and 3-211G (d) basis set calculations. The GaussSum 3 software was used to compute the density of state (DOS).

ARTICLE INFO

Introduction

Phenazone and its metabolites following the discovery of phenazone 120 years ago, the pharmaceutical industry attempted to develop it in three ways. It was chemically changed to produce a more effective combination, a water-soluble derivative for parenteral administration, and a mixture that is removed faster and more consistently than phenazone. The most well-known outcomes of these efforts are aminophenazone, dipyrone, and propyphenazone. Aminophenazone is no longer in use. The other two chemicals differ from phenazone in terms of potency and elimination half-life [1], water solubility (dipyrone is a water-soluble prodrug of methylaminophenazone), and toxicity in general (propyphenazone and dipyrone do not produce nitrosamines in the acidic environment of the 348 stomachs).

Phenazone, propyphenazone, and dipyrone are widely used antipyretic analgesics in various nations across the world (Latin America, many countries in Asia, Eastern Europe, and Central Europe). Dipyrone has been linked to agranulocytosis. Even though there appears to be a statistically significant correlation, the incidence is low (1 instance per million treatment sessions) [2, 3]. Stevens-Johnson syndrome, Lyell's syndrome, and shock responses have all been linked to antipyretic analgesics. According to new statistics, the frequency of these incidents is on par with, for example, penicillin [4, 5, 6]. All non-acidic phenazone derivatives are non-inflammatory and have no gastrointestinal or (acute) renal damage. In comparison to paracetamol, dipyrone is safe in excess [7].
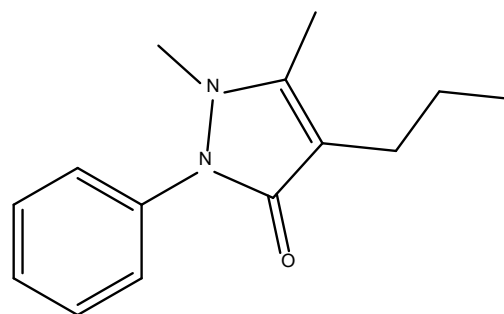
Figure 1. The chemical structure of Phenazone

Paracetamol is regarded as one of the safest antipyretics and analgesics, except for mild hepatotoxicity in rare cases when taken over an extended length of time or in an overdose. Paracetamol is largely processed in the liver into toxic and non-toxic compounds. The molecular structure of phenazone is seen in Figure 1. The molecule is known chemically as N-(4-hydroxyphenyl) ethanamide [8]. Bond lengths, bond angles, and discrepancies between IR and NMR data are analyzed for structural analysis. Quantum chemical characteristics are compared to predict the biological activities of the substances under consideration [9].

Methods

Calculation Method

GaussView 6.0.16 [10] was used to plot the propyphenazone molecule. The Gaussian 09: AS64L-G09RevD.01 software was used for all computations, and an imaginary frequency could not be achieved [11]. In the computations, the HF approach was utilized [12–14]. The base set is chosen as 3–21G (d) [15]. It is possible to approximate quantum chemical descriptors like hardness, softness, chemical potential, and electronegativity using the HF. The following equations were obtained after considering parameters and finite difference techniques to associate the ground state ionization energy and electron affinity values of chemical compounds [16, 17].

Hartree-Fock Method

The Hartree-Fock assumption is the biggest basic reciprocal system used in practically every quantitative calculation, particularly in chemical sequence calculations [18]. This indicates a shift in Hartree's conduct. For single-electron wave functions, the wave function of multiple electrons is an asymmetric element (slater determination). Because of the normal positions of electrons, the travel of each electron in the spin-orbital interplanetary is free, and it experiences repulsion-repulsion amongst electrons (Coulombic repulsion) [19].

The accurate solution of the Schrödinger equation in the many-electron system cannot be determined using the current mathematical technique. HF techniques were developed to approach solving the time-independent Schrödinger equation. Much of the electronic structure theory is based on the HF theory [20,21].

The Hartree-Fock wave function may be calculated computationally by solving the radial integrodifferential HF equations [22]. Algebraic techniques can also be used. They include converting the one-fermion orbitals into an appropriate collection of analytical basis functions, with the goal of obtaining the numerical Hartree-Fock limit if the basis is large enough and complete about square-integrable functions. The molecular orbitals in molecular polyatomic systems are extended into a set of atomic orbitals, the expansion coefficients of which are the variational parameters. The Hartree-Fock equations are rewritten as the Roothaan-Hall self-consistent field equations [23] in this system.

In addition to the Fermi correlation recognized in the HF model, the instantaneous correlation in electron motions due to mutual repulsion, which is neglected in the HF model's average field picture, is frequently critical to obtaining an accurate description of electronic phenomena in atoms, molecules, and solids. The HF solution frequently accounts for more than 99% of total electronic energy in atomic and molecular systems and has a 95% overlap with wave functions derived using more advanced approaches. The 5% remaining in the latter situation is difficult to quantify and can have a significant impact on observables other than energies, such as isotope shifts, hyperfine structures, and transition probabilities [24].

The Hartree-Fock approach is frequently used to provide an approximation of excited states that do not have the lowest symmetry [24]. In this example, stationary energy is calculated by selecting the orbital solution with the necessary number of radial nodes [24]. Although the HF technique can not provide the accuracy necessary today in the description of nuclei, atoms, and molecules, it is frequently employed as the starting point for numerous more sophisticated methods [25, 26].

Spectroscopy

Spectroscopy is the study of the absorption and emission of electromagnetic radiation by atoms and molecules in their gas, liquid, or solid states [27]. Although the terms light, radiation, and electromagnetic radiation can all be used interchangeably, visible electromagnetic radiation is referred to as light. Since the quantum mechanical description of molecular properties [28], spectroscopy has played an important role in the development of quantum mechanics and is fundamental to understanding molecular characteristics. It is also a technique for determining the structure of a substance by the investigation of the interaction of matter and electromagnetic radiation, such as infrared, ultraviolet-visible, and nuclear magnetic resonance spectroscopy. Understanding the characteristics of the molecule is critical for understanding the interaction between matter and electromagnetic radiation. This will provide us with information about the molecule's structure and physical characteristics.

Result and Discussion

Geometry Optimization

Geometry optimization, in its most basic form, is a two-step procedure that predicts the three-dimensional spatial arrangement of atoms in a molecule. The ideal molecular shape of the propyphenazone molecule was calculated using the 3-21G level and is displayed in Figure 2.
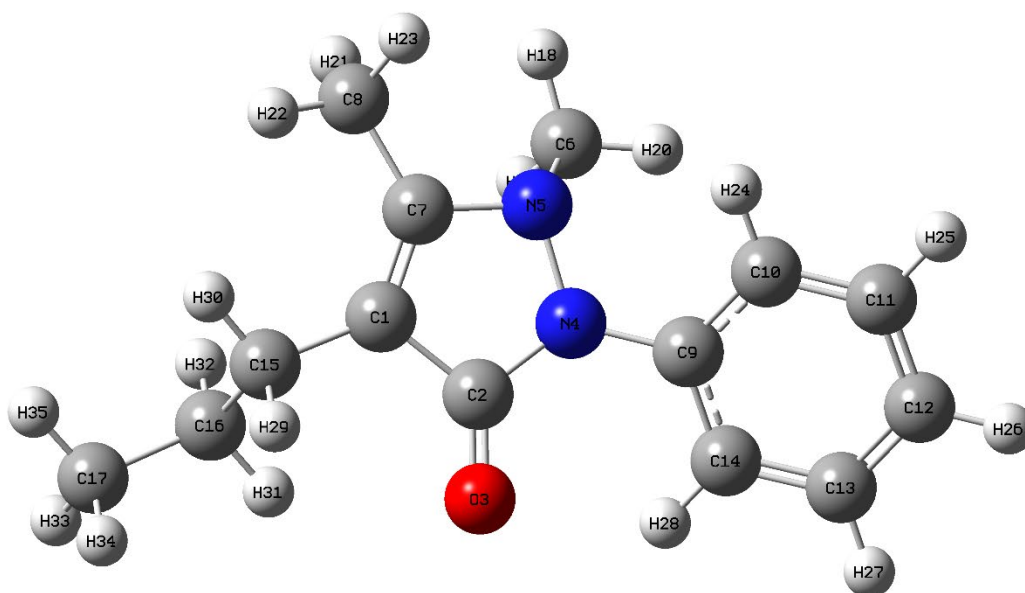
Figure 2. The optimized structures of Propyphenazone molecule

Frontier Molecular Orbital Analysis

The HOMO and LUMO orbital energies can be used to compare molecules' electron-donating and electron-accepting abilities. It has been shown that the HOMO orbital indicates electron-donating capacity and that high values correspond to a good inhibitor. Low LUMO molecular orbital energy and large energy gaps between HOMO and LUMO orbitals suggest that the molecule does not wish to contribute electrons and that electron exchange is simple.

The quantum chemical parameters hardness, softness, and polarizability can be lighted in the light of numerical values with electronic structural principles of the molecule's activity behaviors. Chemical hardness is defined as a molecule's resistance to electron cloud polarization or deformation [29]. Pearson defines hard molecules as having an energy gap between the high-energy HOMO and LUMO orbitals. The geometries of the HOMO and LUMO molecular orbitals reveal that the compounds' electron-donating orbitals are distinct, while the electron acceptor areas may be classified into comparable lobes.

The molecules' global softness is equivalent to the inverse sign of their hardness. Soft, polarizable molecules have a

high level of activity. Electronegativity denotes the electron-withdrawing forces of molecules as well as the chemical potential of electron-donating forces. The electrophilicity index measures a chemical species' proclivity to receive electrons from electron-rich chemical species. The nucleophilicity index measures a chemical species' proclivity to give electrons. In terms of biological activities, compounds with low electronegativity, electrophilicity index, high chemical potential, and nucleophilicity index are more beneficial.

Furthermore, the metrics known as electron donation strength and electron-accepting strength give crucial information about molecules' electron-donating and electron-accepting properties. A chemical with strong biological activity should be able to quickly give electrons. HOMO represents orbitals that may donate electrons, whereas LUMO is an electron acceptor that can collect excited electrons from HOMO. The total energy, energy gap, and dipole moment all have an impact on a molecule's stability. To comprehend the bonding system of the present compound, the surfaces of the border orbitals were drawn.
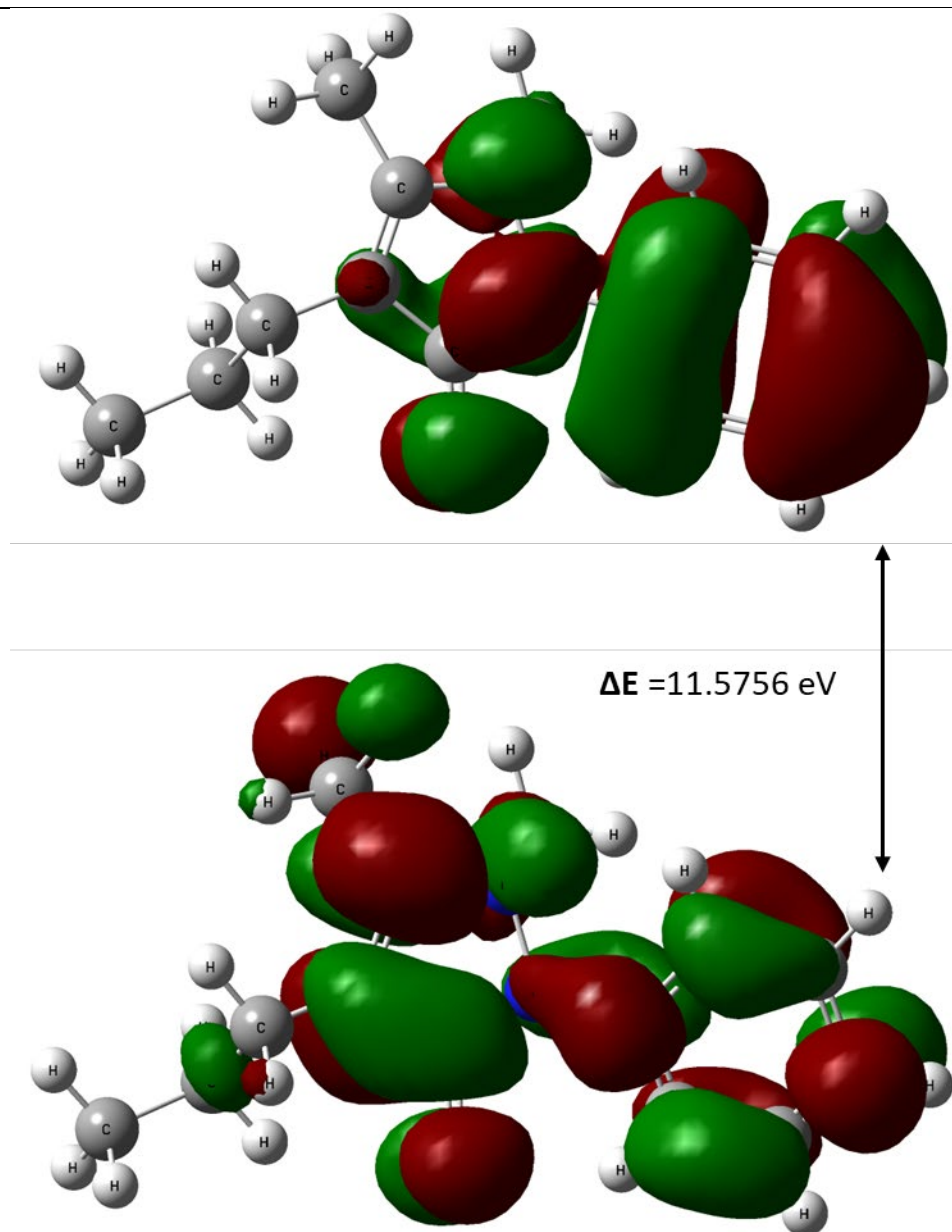
Figure 3. HOMO, LUMO orbitals contour diagram for Propyphenazone molecule

In biological activity studies, quantum chemical parameters such as the highest occupied molecular orbital (HOMO) energy, the lowest unoccupied molecular orbital (LUMO) energy, hardness, softness, chemical potential, electronegativity, electrophilicity index, nucleophilicity index, electron accepting power, and electron donating power play an important role. Table 1 shows the quantum chemical characteristics derived at the 3-21G (d) level for the propyphenazone molecule under consideration.

$$I = -E_{HOMO} \tag{1}$$

$$A = -E_{LUMO} \tag{2}$$

$$\eta = \frac{1}{2}\left[\frac{\partial^2 E}{\partial^2 N}\right]_{v(r)} = \frac{I-A}{2} \tag{3}$$

$$\langle\alpha\rangle = \frac{1}{3}\left[\alpha_{xx} + \alpha_{yy} + \alpha_{zz}\right] \sigma = \frac{1}{\eta} \tag{4}$$

$$\mu = -\chi = \left[\frac{\partial E}{\partial N}\right]_{V(r)} = -\left(\frac{I+A}{2}\right) \tag{5}$$

$$\omega = \frac{\chi^2}{2\eta} \tag{6}$$

$$\varepsilon = \frac{1}{\omega} \tag{7}$$

$$\omega^{+} = \frac{(I + 3A)^2}{16(I - A)} \tag{8}$$

$$\omega^{-} = \frac{(3I + A)^2}{16(I - A)} \tag{9}$$

Table 1. The calculated quantum chemical descriptors for Propyphenazone molecule

Compound	1
E_{HOMO} (eV)	-8.2107
E_{LUMO} (eV)	3.3649
ΔE (eV)	11.5756
η (eV)	5.7878
σ (eV^{-1})	0.1727
χ (eV)	-2.4229
μ (eV^{-1})	2.4229
ω	0.5071
ε	1.9719
ω^{+}	0.0191
ω^{-}	2.4420

Vibrational Spectroscopic Analysis

Molecule infrared spectra are one of the most essential approaches in structural characterization. The IR spectra of the fundamental structures of the propyphenazone molecule were determined at the 3–21G (d) level. Figure 4 depicts the obtained spectra. The vibrational spectra of propyphenazone molecule compounds' peaks were sized.
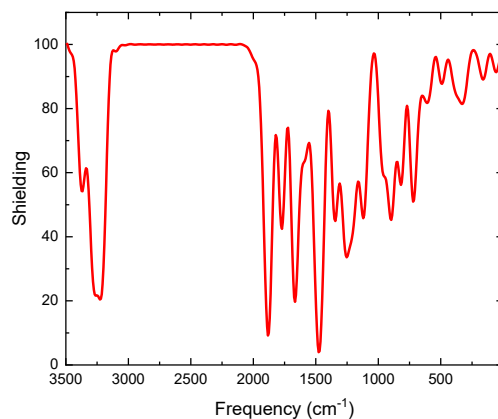
Figure 4. FT-IR Spectrum of at the Propyphenazone Molecule

NMR Spectroscopy

Nuclear magnetic resonance (NMR) is a well-established technique for analyzing complex macromolecules [30]. Magnetic shielding estimates utilizing high-frequency approaches significantly increase the size of molecules [31, 32]. Close electronegative groups diminish the surrounding electron density, concealing the peak location from the external magnetic field and shifting the signal to higher ppm. Chemical shifts may be used to investigate intermolecular effects, and this investigation reveals how electron density and electronegativity of nearby groups impact the chemical shift detected for the molecule. Figure 5 depicts a plotted comparison of computed 13C-NMR chemical shifts at the 3–21G level of examined compounds.

Understanding the NMR spectrum requires the ability to distinguish chemical equivalent and non-equivalent protons in a molecule. We should be able to anticipate how many signals are there in the 1H NMR spectra for the chemical with the specified structure. If, on the other hand, the 1H NMR spectrum of an unknown drug is available, counting the number of signals in the spectrum gives us the number of distinct sets of protons in the molecule, which is critical information for determining the structure of the substance.
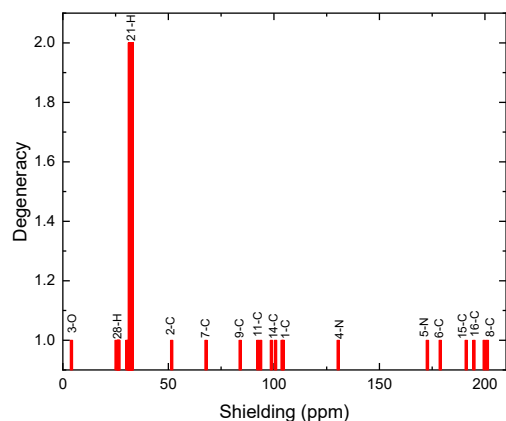
Figure 5. NMR Spectrum of Propyphenazone Molecule

ChemNMR ^{1}H Estimation
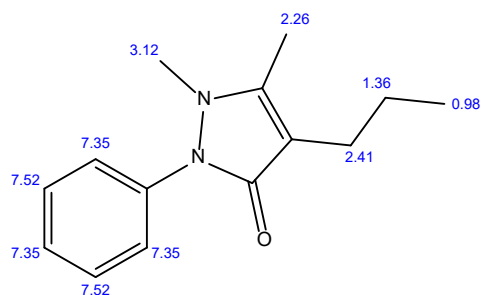
Estimation quality is indicated by color: good, medium, rough

Figure 6. 1H-NMR Spectrum of Propyphenazone Molecule

ChemNMR ^{13}C Estimation
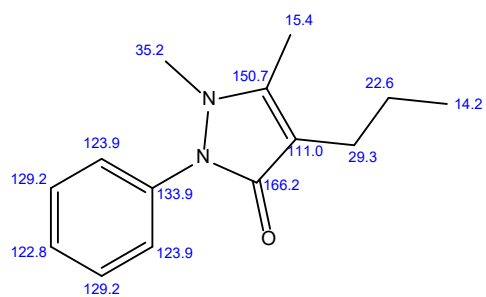
Estimation quality is indicated by color: good, medium, rough

Figure 7. 13C-NMR Spectrum of Propyphenazone Molecule

Because of the non-equivalence of the various carbon atoms, the 13C NMR spectrum of the investigated molecules reveals some prominent peaks corresponding to distinct carbon atoms, as seen in Figure 6. Figure 7 shows that in the case of the propyphenazone molecule, there are virtually

intense peaks with overlapping peak locations. However, in the case of the propyphenazone molecule, only one strong peak arises due to the lack of symmetry in the system. The electro negative's efficiency, on the other hand, is based on far-near and direct-indirect interactions between the electronegative atoms and their nearby carbons.

Because the negatively charged nitrogen atom pulls more electrons from nearby α-carbons, the carbon cores are less shielded. The chemical shift values of the less protected carbon atoms are higher than those of the other carbon atoms in the ring [33].

UV–Visible analysis

The UV-Vis spectra were theoretically synthesized using the time-dependent TD-DFT approach with the 3–21G basis set. The excited states of the propyphenazone molecule were computed using the TD-DFT method. Figure 8 depicts the theoretical UV-visible spectrum of the title chemical. The title molecule's optical absorption maximum, which corresponds to electron transitions between border orbitals, was estimated using molecular orbital geometry calculations.
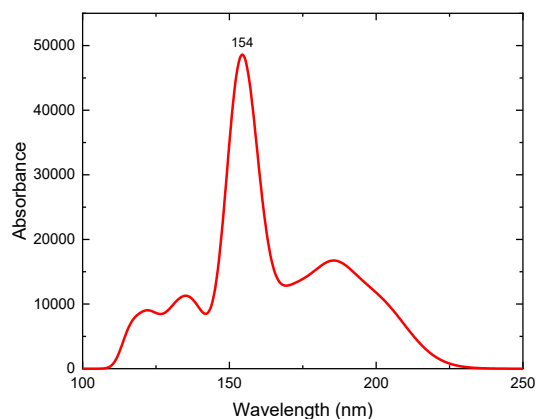
Figure 8. UV-Vis spectra of Propyphenazone Molecule

Molecular Electrostatic potential (MEP)

Electrostatic potential calculations may provide some benefits in analyzing the reactivity of molecules against positively or negatively charged reactants to have a detailed interpretation of their reactivity. Figure 8 depicts the computed Molecular Electrostatic Potential Surfaces. The high-density sections of the electrostatic potential energy values are shown in red in this image, whereas the lowest component is blue [34].
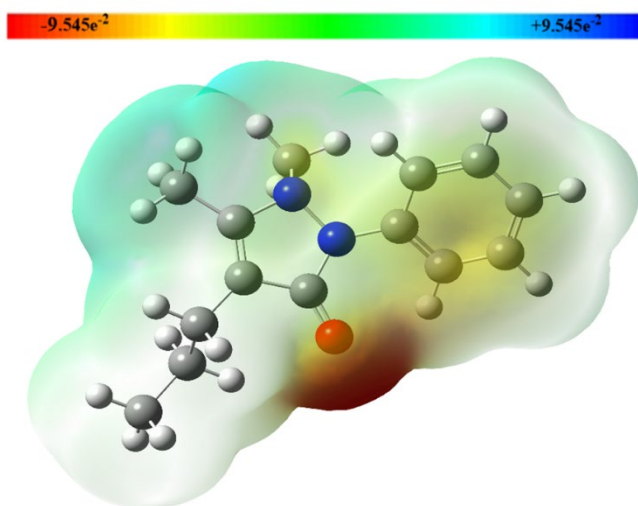
Figure 9. MEP of Propyphenazone Molecule

Figure 10. DOS of Propyphenazone Molecule

Figure 9 depicts 3D plots of the propyphenazone molecule's molecular electrostatic potential (MEP) map with a constant electron density surface. The MEP is a valuable characteristic for investigating the reactivity of approaching electrophiles. Negative places will attract it (where the electron distribution effect is dominant). The maximum negative region chose the site for electrophilic attack indications as the red color in the MEP plot, whereas the highest positive region preferred the location for nucleophilic attack symptoms as the blue color.

The MEP map is significant because it indicates molecule size and structure as well as positive, negative, and neutral electrostatic potential zones in color grading. It is extremely beneficial in the study of molecular structures and the links between their physiochemical properties [35-38]. On the MEPs map, different electrostatic potential levels at the surface are depicted by different colors. When the color shifts from red to blue, the potential grows. The color code maps in the compound range between -0.09545 a.u. (dark red) and 0.09545 a.u. (dark blue), with blue indicating the highest attraction and red indicating the strongest repulsion.

Density of States (DOS)

The approach allows for the density of states to be calculated while recognizing three or four peaks and properly defining their shape and size. Some spectral information located inside a specific limited area cannot be detected successfully. The approach to addressing the inverse issue of rebuilding the function g(ω) allows the degree of ambiguity of the acquired answer to be determined. The Gauss-Sum 3 algorithm was used to compute group contributions to molecular orbitals and generate the density of states spectrum shown in Figure 9.
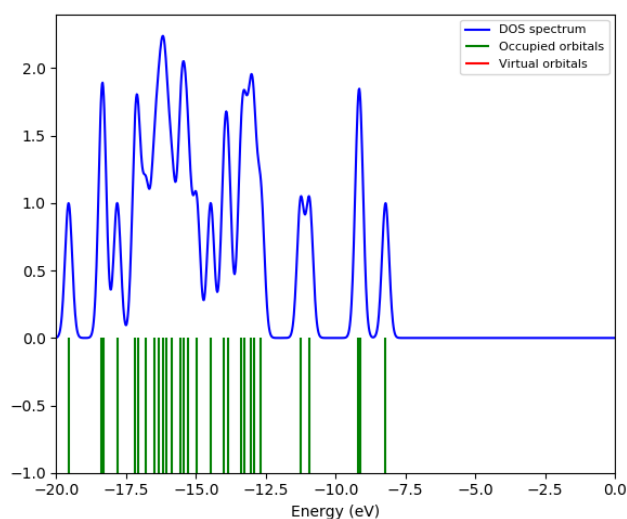
The density of states of the propyphenazone molecule was displayed in Figure 10 to assure an illustrated portrayal of molecule orbital compositions. The Gauss-Sum 3 software was used to calculate the full width at half maximum (FWHM) of 0.3 eV by convoluting molecular orbital information with Gaussian curves of unit height [20]. The DOS spectrum's most important application is to illustrate molecular orbital compositions and their contributions to chemical bonding via the OPDOS spectra. A positive OPDOS score indicates a bonding contact, whereas a negative value indicates an antibonding interaction, and a zero value indicates a nonbonding interaction [39, 40].

Conclusion

The propyphenazone molecular diagram can be described as consisting of an aryl ring that has been fused with two benzene rings and with two pyridine rings, along with two methyl groups attached to the benzene rings. The compounds' fundamental structures were optimized at the 3–21G (d) level. The obtained structural parameters revealed differences in the cyclopentadienyl ring in comparison to the propyphenazone molecule. It was investigated whether the compounds of the propyphenazone molecule were stable. IR and NMR techniques, which are spectroscopic methods, were used in-depth for structural characterization, and the variations in the obtained spectra were compared. Quantum chemical parameters like the highest occupied molecular orbital (HOMO) energy, the lowest unoccupied molecular orbital (LUMO) energy, hardness, softness, chemical potential, electronegativity, electrophilicity index, nucleophilicity index, the electron accepting power, the electron donating power, and polarizability were considered when estimating activity. According to the level of uncertainty, it is predicted that activity will rise. If compounds are isolated, which was the case for propyphenazone and its two propionyl salts, it is clear that the approach will yield results. The propyphenazone

molecule was analyzed using DOS, 1H, and 13C NMR spectroscopy. The HF method with 3–21G (d) basis sets was employed to optimize the geometry. The theoretical values of chemical shifts for 1H and 13C were compared. The absorption wavelengths of the molecule were calculated and the UV-Vis spectra were shown. The results of the HF calculations of the propyphenazone molecule showed good agreement.

Acknowledgments

References

[1] Levy M, Zylber-Katz E, Rosenkranz B 1995 Clinical pharmacokinetics of dipyrone and its metabolites. Clinical Pharmacokinetics 28: 216–234

[2] Ohno H, Yamashita K, Yahata et al 1986 Maternal plasma concentrations of catecholamines and cyclic nucleotides during labor and following delivery. Research Communications in Chemical Pathology and Pharmacology 51: 183–194

[3] Kaufman DW, Kelly JP, Levy M, Shapiro S 1991 The drug etiology of agranulocytosis and aplastic anemia. Monographs in Epidemiology and Biostatistics 18. Oxford University Press, Oxford

[4] Roujeau JC, Kelly JP, Naldi L, Rzany B, Stern RS, Anderson T, Auquier A, Bastuji-Garin S, Correia O, Locati F, Mockenhaupt M, Paoletti C, Shapiro S, Sheir N, Schöpf E, Kaufman D 1995 Drug etiology of Stevens–Johnson syndrome and toxic epidermal necrolysis, first results from an international case–control study. New England Journal of Medicine 333: 1600–1609

[5] Mockenhaupt M, Schlingmann J, Schroeder W, Schoepf E 1996 Evaluation of non-steroidal anti-inflammatory drugs (NSAIDs) and muscle relaxants as risk factors for Stevens–Johnson syndrome (SJS) and toxic epidermal necrolysis (TEN). Pharmacoepidemiology and Drug Safety 5: 116

[6] International Collaborative Study of Severe Anaphylaxis 1998 Epidemiology 9: 141–146

[7] Wolhoff H, Altrogge G, Pola W, Sistovaris N 1983 Metamizol—akute Überdosierung in suizidaler Absicht. Deutsche Medizinische Wochenschrift 108: 1761–1764

[8] Indian Pharmacopoeia 2014, volume II, page 1237; volume III, page 2429 and 2586.

[9] Erkan, S. & Dikyol, D. C. (2022). Computational Structure Characterization of 1,2,3-Selendiazole Isomers, Investigation of Some Molecular Properties and Biological Activities. Cumhuriyet Science Journal, 43 (2), 246-256.

[10] Dennington R.D., Keith T.A., Millam J.M., GaussView 6.0. 16, Semichem. Inc., Shawnee Mission KS, 2016.

[11] Frisch M.J., Trucks G.W., Schlegel H.B., Scuseria G.E., Robb M.A., Cheeseman J.R., Nakatsuji H., Gaussian09 Revision D. 01, Gaussian Inc.,Wallingford CT, 2009. http://www.gaussian.com.

[12] Becke A. D., Perspective: Fifty years of density-functional theory in chemical physics, The Journal of Chemical Physics, 140(18) (2014) 18A301.

[13] Lee C., Yang W., Parr R. G., Development of the Colle-Salvetti correlation-energy formula into a functional of the electron density, Physical Review B., 37(2) (1988) 785.

[14] Zhao Y., Truhlar D. G., The M06 suite of density functionals for main group thermochemistry, thermochemical kinetics, noncovalent interactions, excited states, and transition elements: two new functionals and systematic testing of four M06-class functionals and 12 other functionals, Theoretical Chemistry Accounts, 120(1-3) (2008) 215-241.

[15] Rassolov V.A., Ratner M.A., Pople J.A., Redfern P.C., Curtiss L.A., 6-31G* basis set for third-row atoms, J. Comput. Chem., 22 (9) (2001) 976–984.

[16] EL Aatiaoui, A., Koudad, M., Chelfi, T., ERKAN, S., Azzouzi, M., Aouniti, A., & Oussaid, A., Experimental and theoretical study of new Schiff bases based on imidazo (1, 2-a) pyridine as corrosion inhibitor of mild steel in 1M HCl, Journal of Molecular Structure, (2021) 1226 129372.

[17] Al-Otaibi J. S., Mary Y. S., Mary Y. S., Kaya S., Erkan S., Spectral analysis and DFT investigation of some benzopyran analogues and their self-assemblies with graphene, Journal of Molecular Liquids, 317 (2020) 113924.

[18] Young, D., (2004). Computational chemistry: a practical guide for applying techniques to real world problems, John Wiley & Sons, New Jersey, USA.

[19] Sherrill, C.D. (2000). An introduction to Hartree-Fock molecular orbital theory, School of Chemistry and Biochemistry Georgia Institute of Technology, Atlanta, USA.

[20] Lewars, E., (2003). Introduction to the theory and applications of molecular and quantum mechanics, J. Computational chemistry, Ontario Canada.

[21] Onishi, T., (2018). Quantum Computational Chemistry, Modelling and Calculation for Functional Materials, Springer Nature, Singapore.

[22] Froese Fischer, C (1977). The Hartree-Fock Method for Atoms: A Numerical Approach John Wiley and Sons, New York. ISBN 047125990X.

[23] Helgaker, T; Jørgensen, P and Olsen, J (2000). Molecular Electronic-Structure Theory Wiley, Chichester. ISBN 0471967556.

[24] Froese Fischer, C; Brage, T and Jönsson, P (1997). Computational Atomic Structure: An MCHF Approach, Institute of Physics, Bristol. ISBN 0750304669

[25] Shavitt, I and Bartlett, R-J (2009). Many-Body Methods in Chemistry and Physics: MBPT and Coupled-Cluster Theory Cambridge Molecular Science Cambridge University Press, Cambridge. ISBN 9780521818322

[26] Ring, P and Schuck, P (2000). The Nuclear Many-Body Problem Springer-Verlag, Berlin, Heidlberg. ISBN 3-540-09820-8.

[27] McHale, J.L., (2017). Molecular spectroscopy, Taylor & Francis Group, New York, USA.

[28] Perkampus, H.-H., (2013). UV-VIS Spectroscopy and its Applications, Springer-Verlag Berlin Heidelberg, Germany.

[29] Kaya S., Kaya C., A new method for calculation of molecular hardness: a theoretical study, Computational and Theoretical Chemistry, 1060 (2015) 66-70.

[30] Knicker, H., Almendros, G., González-Vila, F.J., Lüdemann, H.-D., and Martin, F., 13C and 15N NMR analysis of some fungal melanins in comparison with soil organic matter, Organic Geochemistry, 23(11-12), (1995) 1023-1028.

[31] Cheeseman, J.R., Trucks, G.W., Keith, T.A., and Frisch, M.J., A comparison of models for calculating nuclear magnetic resonance shielding tensors, The Journal of chemical physics, 104(14), (1996) 5497-5509.

[32] Frisch, M., Trucks, G., Schlegel, H., Scuseria, G., Robb, M., Cheeseman, J., Zakrzewski, V., Montgomery Jr, J., Stratmann, R.E., and Burant, J., (1998). Gaussian 98, revision a. 7, Gaussian, Inc., Pittsburgh, PA, 12.

[33] Khalid HH, Erkan S, Bulut N, Halogens Effect on Spectroscopy, Anticancer and Molecular Docking Studies for Platinum complexes, Optik (2021).

[34] Erkan, S., Kaya, S., Sayin, K., & Karakaş, D. Structural, spectral characterization and molecular docking analyses of mer-ruthenium (II) complexes containing the bidentate chelating ligands. Spectrochimica Acta Part A: Molecular and Biomolecular Spectroscopy, 224, (2020) 117399.

[35] J.S. Murray, K. Sen, Molecular Electrostatic Potentials, Concepts and 399 Applications, Elsevier, Amsterdam, 1996.

[36] E. Scrocco, J. Tomasi, in: P. Lowdin (Ed.), Advances in Quantum Chemistry, Academic Press, New York, 1978, 402.

[37] J. Sponer, P. Hobza, Int. J. Quant. Chem.,1996, 57, 959–970

[38] F.J. Luque, M. Orozco, P.K. Bhadane, S.R. Gadre, J. Phys. Chem.,1993, 97, 9380–9384.

[39] M. Chen, U.V. Waghmare, C.M. Friend, E. Kaxiras. J. Chem. Phys.,1998, 109, 6854–6680.

[40] E.B. Sas, M. Kurt, M. Can, S. Okur, S. İcli, S. Demic, Structural investigation of a self–assembled monolayer material 5–[(3–methylphenyl) (phenyl) amino] isophthalic acid for organic light–emitting devices, Spectrochimica Acta Part A: Molecular and Biomolecular Spectroscopy (2014)